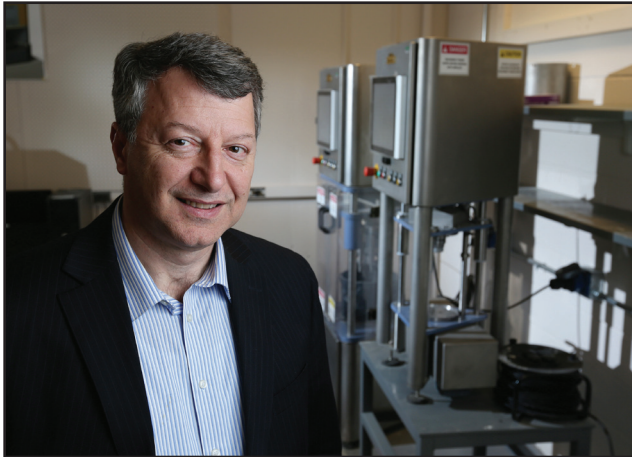


From the desk of the Director



CTIS Director K. H. Khayat with newly acquired state-of-the-art concrete rheometers

As the flowers and trees begin to blossom on the Missouri S&T campus, the CTIS faculty, staff and students are preparing for the completion of several research projects within the CTIS program, some of which are highlighted in this issue. The CTIS team is also taking the next steps to spring into the subsequent level of transportation infrastructure research activities. As a result of the efforts of a team of researchers led by CTIS Director, Kamal H. Khayat, **Advanced Materials for Sustainable Infrastructure** has been identified as a signature area of research in which Missouri S&T can be positioned to become a national leader. As part of the University's commitment to this strategic initiative, new funding has been made available from campus and the University of Missouri System to support the hiring of additional faculty in this interdisciplinary area, as well as in other areas of strategic importance.



In this issue:

From the desk of the Director

Non-destructive evaluation of bridge decks - part 2

Advanced moisture modeling of polymer composites

Advanced Construction Materials Laboratory Inauguration

Analysis of carbon emission regulations in supply chains with volatile demand

Nano-engineered polyurethane resin-modified concrete

Dilation behavior and strain rate effects of rubberized concrete confined with fiber reinforced polymers

Optimization of rheological properties of self-consolidating concrete by means of numerical simulations to avoid formwork filling problems in presence of reinforcement bars

Shear wave velocity measurement of fresh concrete with bender element



PROJECT UPDATE:

Non-destructive evaluation of bridge decks - part 2

- Dr. Norbert H. Maerz, Program Head, Geological Engineering, Missouri S&T



Figure 1. LIDAR scanner set up to scan a Missouri bridge after hydro-demolition used to remove unsound concrete

In the Summer 2013 news issue (Vol. 8, Issue 1), Drs. Leslie Sneed and Neil Anderson presented a non-destructive method of determining the soundness of bridge decks using Ground Penetration Radar (GPR). GPR data when processed can provide a map of the soundness of the bridge deck. GPR data were acquired on a number of bridge decks in Missouri. These decks were subsequently subjected to hydro-demolition using high pressure water jets. This process preferentially removes the deteriorated concrete while leaving intact the sound concrete. A good spatial correlation is expected between the areas where concrete was removed by hydro-demolition

and where the concrete is reported as highly deteriorated by the GPR survey.

To verify the accuracy of the GPR method, a Light Detection and Ranging (LIDAR) scanner was used to measure the depth and volume of the material removed. (Figure 1). The scanner can very precisely measure the topography of surface of the road and consequently the depth of concrete removal (Figure 2). This is done by conducting before (hydro-demolition) and after LIDAR scans, to create a map of the difference in depth readings of the materials removed.



Non-destructive evaluation of bridge decks - part 2 (continued)

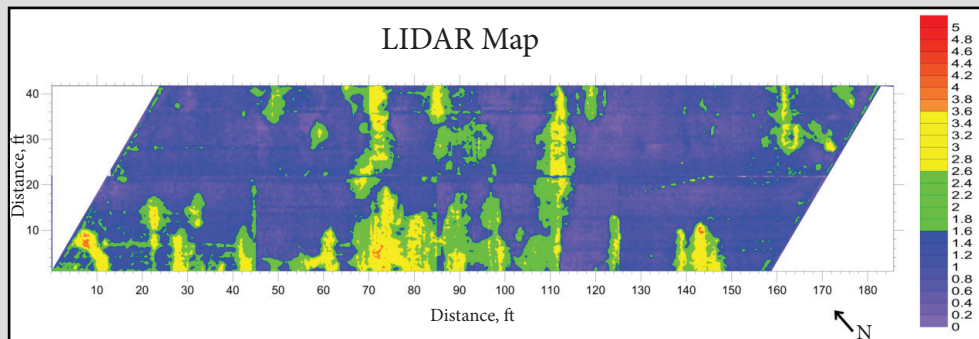


Figure 2. LIDAR map of a span of the Union Pacific railroad bridge (A1298) on Highway 50 in Missouri. Blue areas show little or no concrete removal, while yellow and red show removal of 3-4” of concrete before reaching sounds material.

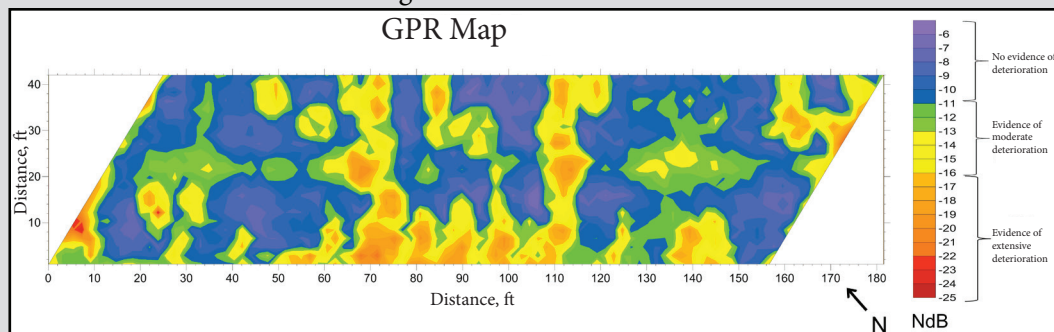


Figure 3. GPR map of the same span of the Union Pacific railroad bridge (A1298) on Highway 50 in Missouri. Blue areas predict minor deterioration, while orange and red areas predict extreme deterioration. Courtesy of Dr. Neil Anderson

This “depth of removal” map can then be compared to a registered image of the GPR survey (**Figure 3**), which shows the areas in which we would expect good concrete and areas in which we would expect poor concrete.

Comparing Figures 2 and 3 shows a very good correlation between the GPR soundness data and the LIDAR map of the depth of material removed.

The average depth of the rebar for both lanes was determined to be 1.76 inches below the original surface.

Average percent of area $\frac{3}{4}$ inch or less in depth	30.2%
Average percent of area $\frac{3}{4}$ inch to top of rebar	47.5%
Average percent of area deeper than top of rebar	22.3%



PROJECT UPDATE:

Advanced moisture modeling of polymer composites

-K. Chandrashekhara, Curators' Professor, Dept. of Mechanical and Aerospace Engineering, Missouri S&T

-N. Roe, Z. Huo, V. Bheemreddy, Dept. of Mechanical and Aerospace Engineering, Missouri S&T

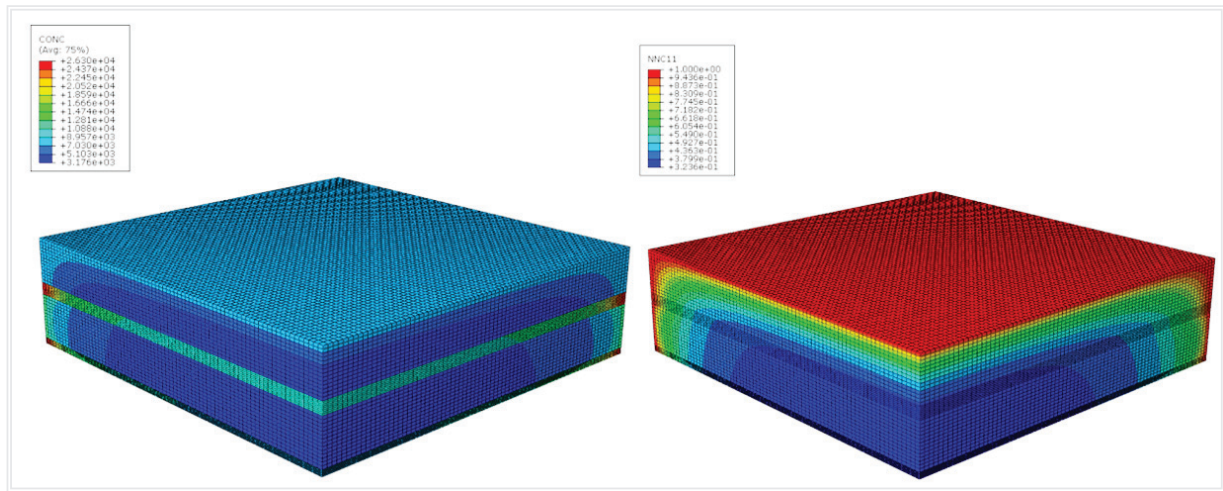


Figure 1. Model of four-layer symmetric hybrid composites with adhesive layers

Long-term moisture exposure has been shown to affect the mechanical performance of polymeric composite structures. This reduction in mechanical performance must be considered during product design to ensure long-term structure survival. In the current work, a three dimensional model is developed and implemented in commercial finite element code. The parametric study has been conducted for 3D shapes, moisture diffusion pathways, and varying moisture and temperature conditions.

The moisture diffusion characteristics in two-phase hybrid composites using moisture concentration-dependent diffusion method have been investigated. The two phases are unidirectional S-glass fiber-reinforced epoxy matrix and unidirectional graphite fiber-reinforced epoxy matrix. A user-defined subroutine was developed to implement this method into commercial finite element code.

Three-dimensional finite element models were developed to investigate the moisture diffusion in hybrid composites. A normalization approach was also integrated in the model to remove the moisture concentration discontinuity at the interface of different material components. The moisture diffusion in the three-layer hybrid composite exposed to 45 °C/84% relative humidity for 70 days was simulated and validated by comparing the simulation results with experimental findings.



Advanced moisture modeling of polymer composites (continued)

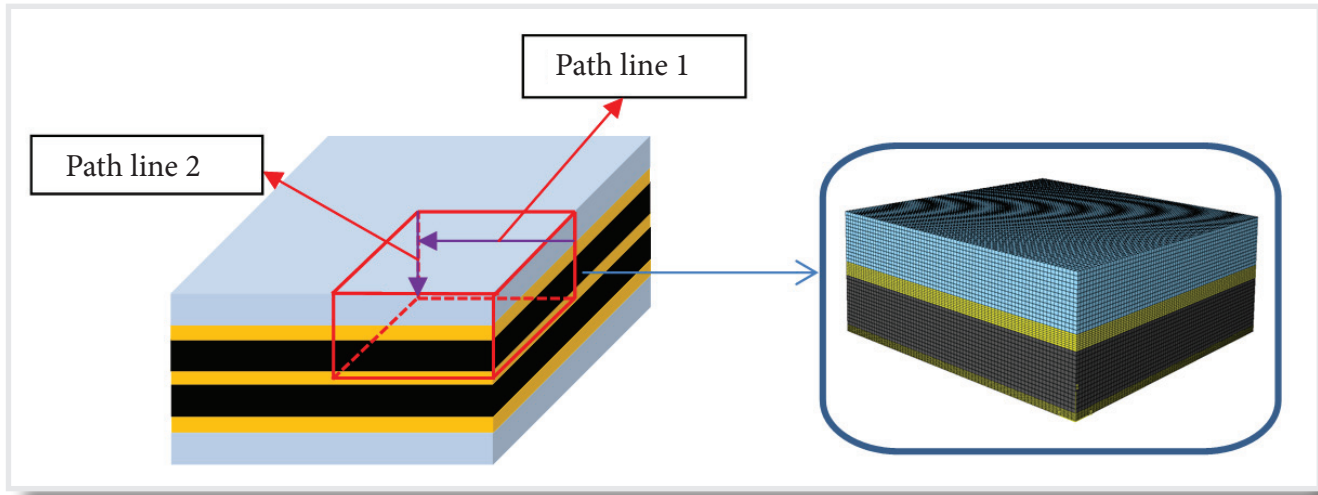


Figure 2. Moisture concentration and normalized concentration contour after 1.5 years of exposure (0.76 mm adhesive)

Results from 2D and 3D models were compared to the analytical and experimental findings. 3D analysis exhibited lower average moisture content in comparison with the prediction from the existing models, but the 3D modeling was more accurate than 2D modeling, especially in prediction of moisture diffusion into thick composite laminates. The results indicated that thinner adhesive layers (0.12 mm thick) did not significantly affect the overall moisture uptake. Thicker adhesive layers (0.76 mm thick) noticeably accelerated the overall moisture uptake after 81 days of conditioning.

ADVANCED CONSTRUCTION MATERIALS LABORATORY (ACML) INAUGURATION



CTIS celebrated the inauguration of the Advanced Construction Materials Laboratory (ACML) on **Friday, April 25**. The renovated laboratory showcases over 35 recently purchased pieces of specialized equipment. This equipment will enable the development, manufacturing, and implementation of advanced and sustainable materials for transportation infrastructure, with emphasis on concrete. A tour of the new concrete batching plant also took place the previous day, **April 24**.



PROJECT UPDATE:

Analysis of carbon emission regulations in supply chains with volatile demand

- Dincer Konur, Assistant Professor, Dept. of Engineering Mgt. and Systems Engr. Missouri S&T
- James Campbell, Professor, Logistics & Operations Mgt. Area, University of Missouri - St. Louis

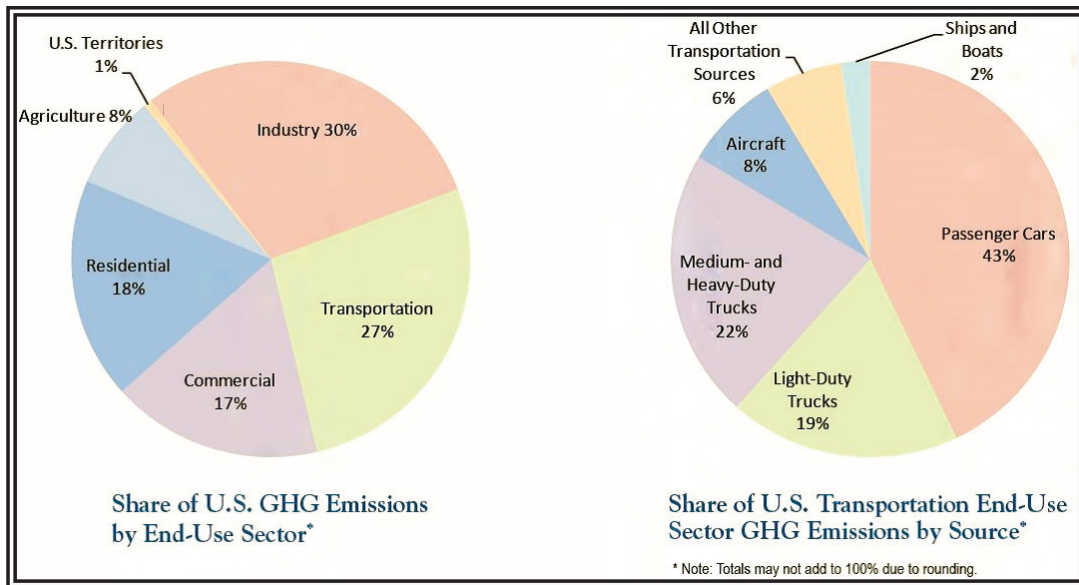


Figure 1. US 2011 GHG Emission Statistics (Source: EPA, 2011)

There is a growing consensus that carbon emissions are a leading contributor to global climate change, which has created increasing pressure around the world to enact legislation to curb these emissions. The US EPA reports that the transportation sector contributed 27% to GHG emissions in 2011 and freight transportation (freight trucks) are major transportation emission source after passenger transportation (see **Figure 1**).

Thus, a very large fraction of carbon emissions is due to supply chain activities including inventory holding, freight transportation, and logistics and warehousing activities. Inventory management is particularly important for a company as this determines not only the level of inventory carried and warehousing activities, but also the amount and the frequency of freight shipments and logistical operations. Hence, the inventory control policy of a company is inextricably linked with its carbon emissions.

The research team (Dr. Dincer Konur from Missouri S&T and Dr. James Campbell from UM-STL) aims at developing decision-making algorithms to help supply chain agents better manage inventory and transportation operations in light of economic and environmental pressures in the presence of demand volatility. To this end, the research team modeled a supply chain agent's stochastic inventory control and transportation planning problem under two well-known proposed carbon emission regulations: carbon-taxing and carbon-cap-and-trade. In this model, delivery speed is explicitly considered. Particularly, speeding the delivery may increase or decrease carbon emission generation rate of transportation while it may also increase or decrease vulnerability of the supply chain agent to the demand volatility. Currently, the research team is working on optimally solving this model. Later, the effects of transportation emissions and delivery speed on costs incurred and emissions generated will be analyzed.



PROJECT UPDATE:

Nano-engineered polyurethane resin-modified concrete

-K. Chandrashekhara, Curators' Professor, Dept. of Mechanical and Aerospace Engineering, Missouri S&T

-J. Volz, Assistant Adjunct Professor, Dept. of Civil, Architectural and Environmental Engr., Missouri S&T

-T. Schuman, Associate Professor, Dept. of Chemistry, Missouri S&T

-G.S. Dhaliwal, Dept. of Mechanical and Aerospace Engineering, Missouri S&T



Figure 1. Flexure test of PMC beam

The goal of this study was to investigate the application of nano-engineered polyurethane (NEPU) emulsions for polymer modified concrete (PMC). NEPU emulsions are non-toxic, environment friendly, durable over a wide temperature range; provide better adhesion, high strength, less cracking, and compatible with all mortar types. One of the weak links in a cement-aggregate composite material is the bond between the matrix and the aggregates. To improve the performance of the alternative cement binder (ACB), the research team intends to develop a NEPU

resin to act as an intermediary between the aggregates and the ACB matrix. The NEPU can be used to precoat the aggregates prior to their placement within the ACB matrix.

To improve the strength of concrete, the research team investigated the effects of introducing polyurethane (PU) and poly (vinyl alcohol co-ethylene) to act as an intermediary between the aggregates and the cement matrix. The polymers used were pre-coated to the aggregate prior to the placement of the aggregate in the cement matrix. The proposed

modified concrete specimens were subjected to compression and flexure tests. In this work, effects of different methods of making polymer modified concrete and the effects of different amounts of polymer were also investigated. The results showed that addition of poly (vinyl alcohol co-ethylene) can improve the flexural strength of the concrete whereas PU had negative effect on the flexural strength of the concrete. Also, the addition of polyurethane and poly (vinyl alcohol co-ethylene) exhibited has a negative effect on the compressive strength of the modified construction.

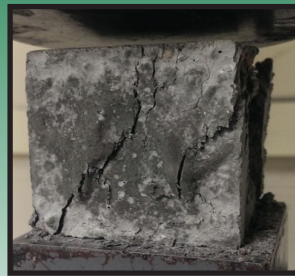


Figure 2a.
Poly (vinyl alcohol co-ethylene)
based concrete specimen

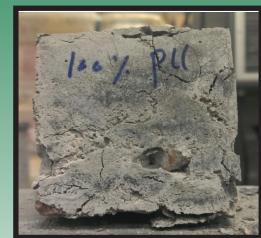


Figure 2b.
Polyurethane
based concrete specimen



PROJECT UPDATE:

Dilation behavior and strain rate effects of rubberized concrete confined with fiber reinforced polymers

- Mohamed ElGawady, Assoc. Professor, Dept. of Civil, Architectural and Envir. Engr., Missouri S&T
- Ayman Moustafa, Graduate Student, Dept. of Civil, Architectural and Envir. Engr., Missouri S&T

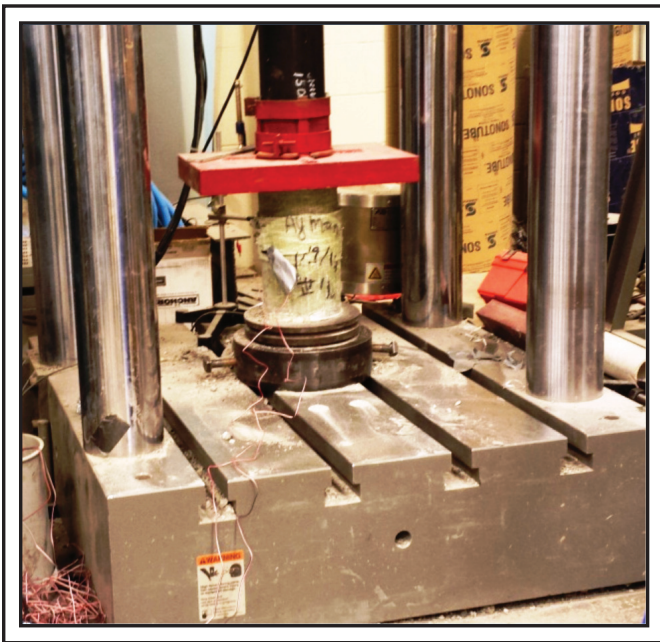


Figure 1. Test setup for compressions testing

Three concrete mix designs including 0%, 10%, and 20% of crumb rubber as a replacement of fine aggregates were designed. A total of 18 concrete cylinders confined with one and three layers of GFRP tubes of normal and rubberized concrete were tested under three different strain rates of $2.8E-5$, $2.8E-3$, and $2.8E-2$ in./in./sec, corresponding to static loading, earthquake loading, and higher shock, respectively. The test setup is shown in **Figure 1**.

The effect of the loading rate on the confined compressive strength (f'_{cc}) in both normal and rubberized concrete is shown in **Figures 2 and 3** (see next page) for concrete confined with one layer and three layers of GFRP, respectively. **Figure 2** shows a linear increase in strength of rubberized concrete confined with one layer of GFRP. For conventional concrete confined with one layer of GFRP, no increase in strength was observed up to a strain rate of $2.8E-3$ in/in/s, beyond that, an increase of 13.9% was observed.

For the concrete confined with three layers of GFRP, shown in **Figure 3**, an increase in confined compression strength is observed from the static rate of $2.8E-5$ in./in./s to the dynamic rate of $2.8E-3$

This project investigates the dilation behavior and effects of strain rate on the behavior of rubberized concrete confined with glass fiber reinforced polymers (GFRP). Rubberized concrete includes scrap-tire rubber as a partial replacement of mineral aggregates which promotes the green construction. The rubber is an elastomeric material and its properties are highly dependent on the type of loading applied; whether it is static or dynamic. The effect of loading type is also inherent in the concrete itself and the properties of concrete are dependent on the strain rate.

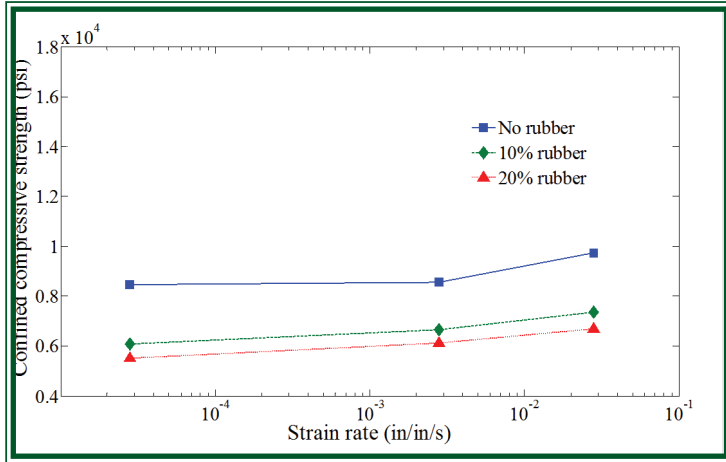


Figure 2. Effect of strain rate on normal and rubberized concrete confined with one layer of GFRP

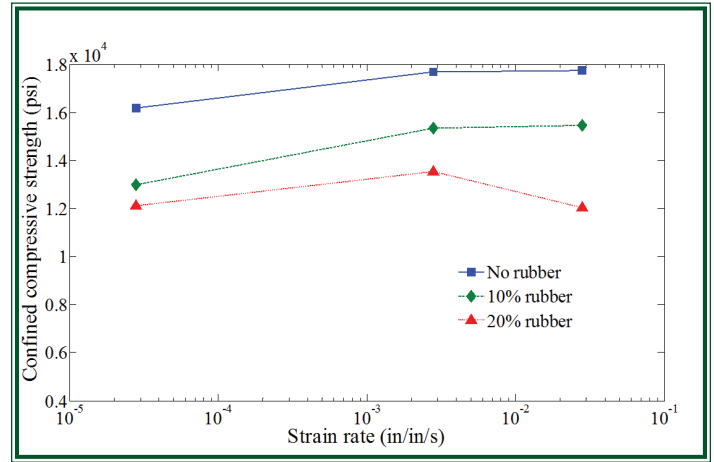


Figure 3. Effect of strain rate on normal and rubberized concrete confined with three layers of GFRP

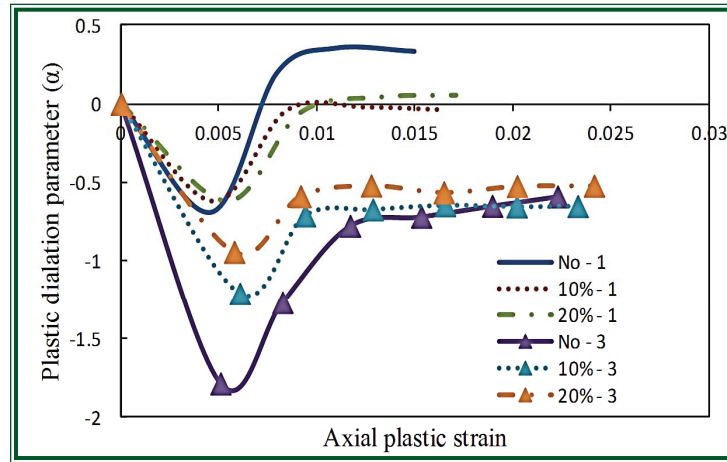


Figure 4. Dilation rate of normal and rubberized concrete

in./in./s and then it stabilizes, which indicates the GFRP is used to its full capacity in confinement and the concrete reached its maximum strength.

Another property of interest in the rubberized concrete is the dilation of concrete represented by the plastic dilation parameter (α), also called dilation rate. The dilation rate of confined concrete is important because it explains the behavior of concrete whether it is contracting or expanding leading to understanding of the effectiveness of confinement. **Figure 4** shows the change of the dilation rate with the axial plastic strain. For the normal concrete with one layer of GFRP, the concrete exerted contraction at the beginning of the loading and then it was dilated into expansion and stabilized. For rubberized concrete, the concrete recovers the dilation and starts to contract again until rupture of FRP occurred. This smooth transition provided by the rubber is due to the higher deformability of rubber and the smooth transition is favorable because it reduces the concrete micro cracks in the transition zone. For confinement with three layers of GFRP, higher initial contraction took place followed by change in dilation rate but without expansion and then recovery of the contraction up to a stabilization point. Again, the favorable smooth transition can be observed for the rubberized concrete.



PROJECT UPDATE:

Optimization of rheological properties of self-consolidating concrete by means of numerical simulations to avoid formwork filling problems in presence of reinforcement bars

- Dimitri Feys, Assistant Professor, Dept. of Civil, Architectural and Environmental Engr., Missouri S&T
- Joontaek Park, Assistant Professor, Dept. of Chemical and Biochemical Engineering, Missouri S&T

In this project, the flow of self-consolidating concrete (SCC) in formwork was simulated using COMSOL Multiphysics® to study the effect of the reinforcement rebar configuration on the flow pattern as well as to find critical rheological properties for adequate formwork filling. Since SCC is a relatively new type of concrete which does not require mechanical consolidation, the flow pattern of SCC in the formwork can significantly influence the mechanical properties of concrete. Especially, the occurrence of dead zones during formwork filling can entrap air and can induce lower mechanical properties and durability of the final structural elements. Dead zones also increase the risk of casting joints or cold joints, thus reducing the bond strength between the concrete layers.

Instead of performing large-scale experiments with large quantities of concrete, the flow in formworks can also be predicted by means of numerical, single fluid simulations, in which the concrete is assumed to be a fluid without particles. However, numerical simulations that take into consideration the influence of reinforcement on local patterns in SCC flow have not been reported extensively. Preliminary simulations have shown that a vertical bar creates additional zones with very low and very high shear rates, compared to the flow in non-reinforced elements.

The SCC is modeled as a single phase yield-stress fluid in a rectilinear channel (length = 1 m, width = 0.4 m) with cylindrical objects. For the influence of the reinforcement configuration, four different rebar configurations were chosen in terms of concrete cover (distance between rebar and wall: d_w) and the distance between the Rebars in flow direction (d_p) (see Table 1). Both the concrete cover and the distance between rebars are determined by structural requirements. As a result, only the concrete rheological properties can be varied to avoid the occurrence of dead zones. For each configuration, the rheological properties (plastic viscosity and yield stress) of the SCC were optimized to find the maximum yield stress to ensure dead zones are minimized and the formwork is filled adequately.

Cases	d_w (m)	d_p (m)	Description
Case A-1	0.025	0.1	Small d_w
Case A-2	0.05	0.1	Large d_w
Case B-1	0.0375	0.05	Small d_p
Case B-2	0.0375	0.25	Large d_p

Table 1. Rebar configuration and description of each case

- Continued Next Page -



Optimization of rheological properties of self-consolidating concrete by means of numerical simulations, to avoid formwork filling problems in presence of reinforcement bars (continued)

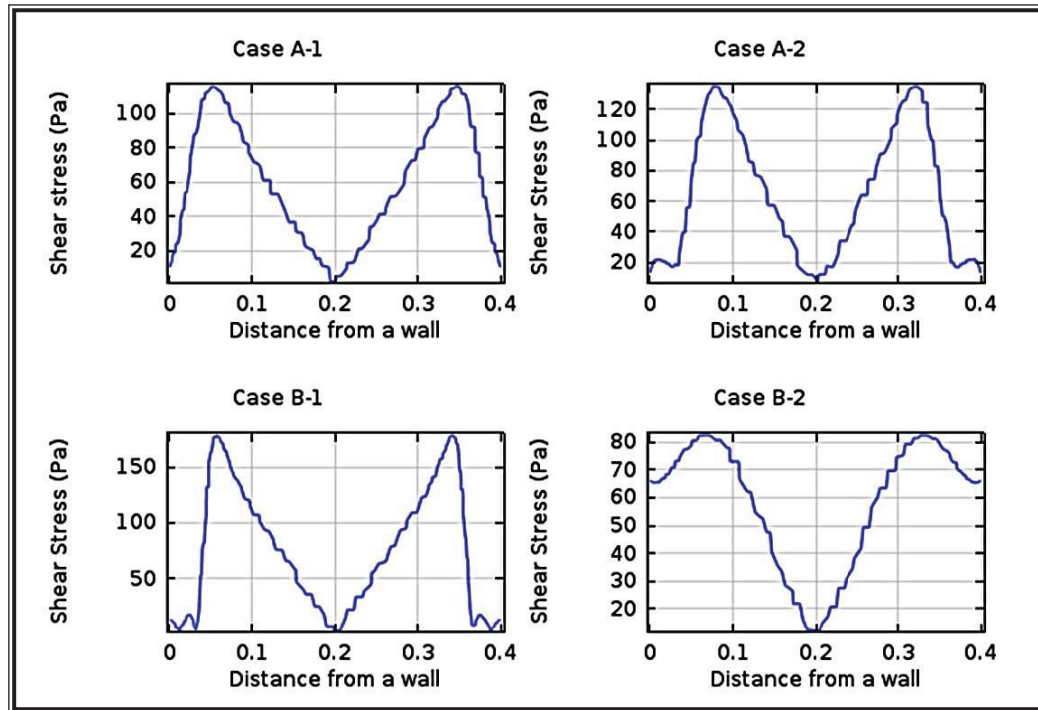


Figure 1. Simulated shear stress (τ^*) profile as a function of the distance from the left side of formwork wall (total width of 0.4m)

The numerical simulations indicated that for the studied cases the spacing between the rebars (d_p) is the most critical parameter for the occurrence of dead zones. The maximum yield stress of the concrete for which no dead zones occurred in case B-1 was significantly lower (3 Pa) compared to the other cases (9-12 Pa). Further analysis of the calculated results revealed that rebars with a small interspacing create some kind of virtual wall, and the shear stress between the rebars and the formwork (i.e. in the concrete cover) is rather low. In **Figure 1**, the shear stress profiles over the thickness of the formworks can be seen. The shear stress is logically zero in the center (at 0.2 m from the walls), while the maximum values are obtained at the position of the rebars. Especially in case B-1, where the rebars are close to each other, the shear stress is almost zero in the concrete cover. Dead zones are thus likely to occur in case B-1, unless self-levelling concrete is used. Dependent on the thixotropic build-up, the self-consolidation may be compromised leading to an increasing quantity of entrapped air. Furthermore, as the rebars create a virtual wall, a cold joint may occur between the concrete at rest in the cover and the concrete moving in the center of the wall, which may reduce the bond behavior between the two concrete layers and between the concrete and the rebars. This could lead to premature deterioration of the concrete cover of our infrastructure.

This project has also shown that numerical simulations can be a quick and easy tool to initially assess optimum concrete properties for specific applications. Performing numerical simulations can save a substantial amount of money, materials and labor to explore specific problems. By means of a short series of experiments, the conclusions of the numerical simulations can be verified and easily implemented in practice.



PROJECT UPDATE:

Shear wave velocity measurement of fresh concrete with bender element

- Bate Bate, Assistant Professor, Dept. of Civil, Architectural and Environmental Engr., Missouri S&T
- Jianfeng Zhu, Graduate Student, Dept. of Chemical and Biochemical Engineering, Missouri S&T

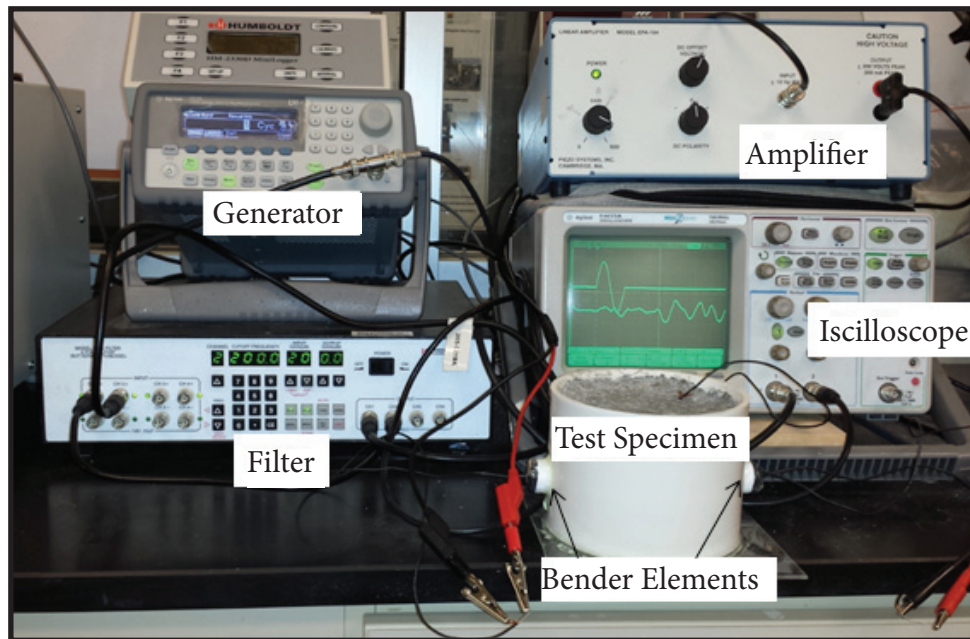


Figure 1. Test Setup

The evaluation of the curing process of concrete is critical to its performance. Traditionally, stress sensor and compressive wave sensor are used to measure concrete properties. Bender element (BE) test, a nondestructive test measuring shear wave velocity (V_s) is widely used in geotechnical engineering. BE test was used to monitor the curing process of fresh concrete in this study.

BE test was performed on a PVC pipe with diameter of 120mm and height of 100mm (Figure 1). The travel distance (tip-to-tip distance) was measured as 103.5mm. The ratio of cement: fine aggregate: coarse aggregate: water was set at 20%: 41%: 30.5%: 8.5% with w/c of 0.425. The density of the mixture was 2180 kg/m³. Both sine

shear wave (30 kHz) and square shear wave (20 Hz) were applied. The frequency cutoff was from 200Hz to 200kHz.

Test result shows the shear wave velocity increased dramatically with time. At the age of 72 hours, V_s was as high as 986 m/s (Figure 2). The measured V_s result is lower than typical values reported in the literature (Table 1). This is primarily due to the short curing period of 3 days.

Assuming Poisson's ratio of 0.2, compressive wave velocity (V_p) and Young's modulus (E) can be calculated by Equations 1-3 (see next page). V_p and E are close to those reported in the literature.



Shear wave velocity measurement of fresh concrete with bender element (continued)

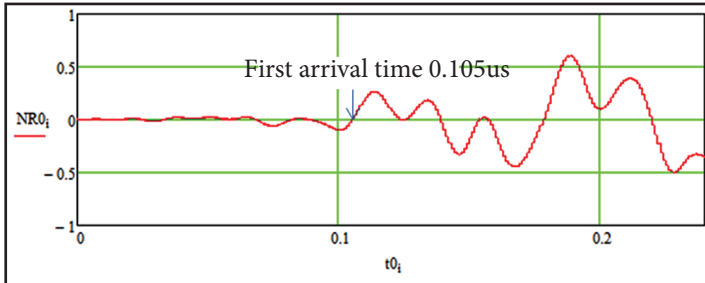


Figure 2. Received signal after 72 hours curing

$$G = \rho V_s^2 \quad (1)$$

$$v = \frac{1 - 2\left(\frac{V_s}{V_p}\right)^2}{2 - 2\left(\frac{V_s}{V_p}\right)^2} \quad (2)$$

$$E = 2\rho V_s^2(1 + v) \quad (3)$$

It worth noting that V_s of cement paste (Zhu et al. 2011) was around 600 m/s, which is lower than concrete. Both sine and square waves yielded similar results. Shear wave velocity from square waves is only 2.7% higher than that from sine waves.

Table 1. Comparison of test results

		V_s (m/s)	V_p (m/s)	ν	E (GPa)	ρ (kg/m ³)	w/c
This study	at 3 days	986	1616 (if $\nu=0.2$)	0.2 (assumed)	5.1 (if $\nu=0.2$)	2180	0.425
Recep (2009)	at 28 days	2417±104	418±38	0.24	28.4	2190	0.45
Malhotra and Carino (2004)	hardened concrete	60% V_p	~4000	-	-	-	-
Zhu et al. (2011)		600 (cement paste at 6 hours)	4010 (hardened concrete)	-	-	-	0.4
Finno and Chao (2005)	hardened concrete	2200-2800 (assumed)	-	0.14-0.28	-	~2350	-
An et al. (2009)	Different curing age	450-2700	-	-	-	-	0.38

References

- Richard J. Finno and Hsiao-chou Chao. (2005) Shear wave velocity in concrete cylinders (piles)—universal mode method. *ACI Materials Journal*, V. 102, No. 3.
- Jinying Zhu, Yi-Te Tsai and Seong-Hoon Kee. (2011). Monitoring early age property of cement and concrete using piezoceramic bender elements. *Smart Mater. Struct.* 20, 115014 (7pp).
- David B. Scott. (2013). Internal inspection of reinforced concrete for nuclear structures using shear wave tomography. *Energy Conversion and Management* 74, 582–586.
- Recep Birgül. (2009). Hilbert transformation of waveforms to determine shear wave velocity in concrete. *Cement and Concrete Research* 39, 696–700.
- Lee, J. and Santamarina, J. (2005). Bender elements: performance and signal Interpretation. *J. Geotech. Geoenviron. Eng.*, 131(9), 1063–1070.
- Mehta, P.K. and Monteiro, P.J.M. (2006). *Concrete: microstructure, properties, and materials*. 3rd edition. McGraw-Hill Companies, Inc., 203-251
- Malhotra VM, Carino NJ. (2004). *Handbook on nondestructive testing of concrete*. 2nd edition. CRC Press.
- Ji-Hwan An, Jeong-Hee Nam, Soo-Ahn Kwon and Sung-Ho Joh. (2009). Estimation of the compressive strength of concrete using shear wave velocity. *Geo-Hunan International Conference 2009*.